Effects of strain rate on hot tear formation in Al-Si-Cu alloys

IOP Conf. Series: Materials Science and Engineering **529** (2019) 012053 doi:10.1088/1757-899X/529/1/012053

Effects of strain rate on hot tear formation in Al-Si-Cu alloys

S Bhagavath[1], B Cai[2], R Atwood[3], PD Lee[4,5], S Karagadde[1*]

[1]Department of Mechanical Engineering, Indian Institute of Technology Bombay, Mumbai 400076, India

[2]University of Birmingham, Edgbaston, Birmingham, B15 2TT UK,

[3]Diamond Light Source, Harwell Campus, OX11 0DE, UK,

[4] Research complex at Harwell, Harwell Campus, OX11 0FA UK, [5]University college of London, London WC1E 6BT, UK

*Corresponding author: **s.karagadde@iitb.ac.in**

Abstract. The alloy casting process is one of the major manufacturing processes to produce near net shape components. The casing process is prone to a wide variety of defects, with hot tear being one of the most detrimental. The two main factors generally recognized as the primary cause for formation of hot tears are the mechanical response of the mush (which effects its permeability), and the solidification range (solidification time). The response of the mushy zone under deformation is mainly affected by the solid fraction, strain rate and grain morphology. Even though the science behind the formation of hot tear is understood, there is no general criterion to quantify the hot tear formation under varying casting conditions. The development of ultra-fast X-ray imaging has facilitated the means to quantify the effects of the critical parameters in-situ and develop better correlations for hot tear prediction. The in situ experiments will also provide insights into mush rheology, which has significant influence on hot tear formation. In this study, isothermal semi solid compression studies of Al-Si-Cu alloys were carried out using specially built thermo-mechanical rig. We studied the effects of the strain rate in the range of 2×10^{-4}– 0.02/s and solid fraction (~0.6-0.9) on the mechanical response of the mushy zone. The sample were characterized before and after deformation using X-ray micro tomography. The data was subjected to an image processing routine and the amount of porosity and hot tear was quantified. The stress-strain curve of the semisolid alloys showed a characteristic strain softening behaviour for semi solid samples with ~0.6-0.7 solid fraction, irrespective of loading rates, whereas the behaviour at higher fractions were that of constant flow stress. Additionally, in situ compression experiments were carried out, wherein the liquid channel thickness at various strain values were measured. Isolated liquid channels were formed under loading, from where the hot tears were found to nucleate. Hot tear susceptibility was found to increase with increasing strain rate and rheology of the mush, which is dependent on solid fraction.

1. Introduction

To achieve the continuing stride for improving the fuel economy and reducing the carbon footprint, development of lightweight high strength alloys for automobiles have become a necessity[1]. The mechanical properties of these alloys is controlled by the microstructure and the solidification defects like hot tear [2][3], segregation[4], porosity[5] etc. The root cause of the defects can be traced to the semi-solid state during solidification, at relatively high solid fractions. At these solid fractions, a solid network is formed and as a consequence, the permeability of the mushy zone will decrease resulting in difficulty in feeding. The response of this network under mechanical deformation has a role in the formation of afore mentioned defects

Both laboratory and *in situ* semi-solid deformation tests have been extensively reported in literature which describes the behaviour of several aluminium alloys under various form of deformation loads, deformation rates, alloy composition and solid fraction. While strength and ductility of the network was determined by conducting tensile tests [6], the rheology of the semi-solid mush is studied by conducting shear [7] and compression. The rheological behaviour of various aluminium alloys at different solid

fractions and strain rate were studied by Kim et al [8], Kang et al [9], Kapranos et al[10] and reported liquid segregation and cracks at the edge of the specimens. Parametric study of semi-solid compression test of Al-4 wt.% Cu alloys to understand the effect of solid fraction, strain rate, grain morphology is reported by Tsimas and identified different factors affecting the flow resistance[11].Based on these experimental observations, several theories of micro-mechanisms of defect formation have been proposed and criteria for cracking have been developed [12][13].

In this work, semi-solid compression experiments of Al-Si-Cu die-cast alloys at different strain rates has been performed. The deformed sample was characterised using 3d tomography to observe the crack morphology. The interplay between the deformation rate and dilatancy is studied from the stress strain diagram.

2. Materials and Methods

Die cast aluminium alloy ADC12, and a modified ADC12 (MADC12) alloy with copper content increased to 10 wt. % was used in the study. The modified alloy was used as to achieve an enhanced contrast between the primary phase and the inter-dendritic liquid. A secondary objective of modifying the alloy was to investigate the influence of the change in freezing range on hydrogen pore growth and the susceptibility of hot tear. The chemical composition of the alloy was assessed using inductively coupled plasma atomic emission spectroscopy (ICP-AES) technique and the major elements are reported in Table 1.

Table 1: Chemical assay of the alloys under study

Sample	Cu (%)	Fe (%)	Si (%)
ADC12	1.82	0.74	11.9
Modified ADC12	10.426	0.794	10.5

The sample alloys were machined into 3 mm diameter cylinders using wire electro discharge machining (EDM). The length of the sample was 5.4±0.3 mm. The Scheil solidification model in Thermocalc® was used to obtain the exact freezing range for determining experimental conditions, and is shown in figure 1(a).

2.1 Test setup

The semisolid compression tests were performed in the bespoke P2R mechanical compression test rig fitted with proportional integral derivative (PID) controlled resistance furnace. The P2R is custom made testing machine that had been used for conducting a variety of semisolid deformation experiments as reported in [14]. The setup has the capability of applying a maximum load of 500N, at a minimum strain rate of 0.1µ/s. The resistive furnace is powered by a high current DC power supply and the temperature is controlled by a Reconfigurable Input Output (RIO) controller (National Instruments, Model –NI cRIO-9068) The furnace can reach a maximum temperature of 1100°C and the temperature can be raised at a maximum rate of 1°C /s. K type thermocouple is used to record and control the furnace temperature. During the semisolid compression, the sample is heated to pre-determined isothermal temperature. A preload of approximately 7 N was applied to keep the sample in place during compression experiments. The loading ram was adjusted during the experiment to account for thermal expansion during heating and preload is maintained. The thermal cycle followed during the experimentation along with the setup and sample arrangement is represented in figure 1(b).

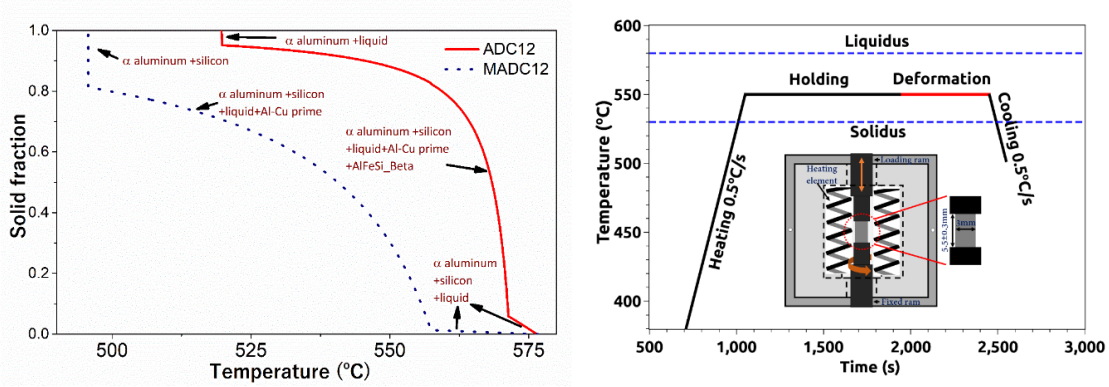

Figure 1: (a) Solid fraction change with temperature for (1) Modified ADC12 (2) ADC12 alloy calculated using Thermocalc® Scheil solidification module (b) Thermal cycle followed during Compression test. Inset- furnace used for the semis solid compression experiment with sample dimensions.

2.2 Post deformation X-Ray tomography characterization

The deformed sample were investigated using 3D using Nikon XT H 225 ST, X-ray tomography machine to know the morphology and distribution of pores. The voltage of the X-Ray source for the ADC-12 samples was set between 70-85kV, whereas for the modified alloy it was between 70-92kV. The sample scan was taken at 40.3 magnification with voxel size of 3.72µm. 3143 projections were taken within 360° with a projection at every 0.116° angle . The exposure time for each scan was 500ms. Flats and darks were taken to minimize the artefacts. The reconstruction of the scan was done using CT agent software, which uses filtered back projection algorithm. The image stacks from the reconstruction was subjected to 3D anisotropic diffusion filter followed by median filter in Fiji Imagej [15]. The initial volume was cropped in to a suitable representative volume. The cropped volume was segmented using Trainable weka segmentation tool [16], a Fiji-Imagej plugin to distinguish porosity and Si particles.

3. Results and Discussion

The radiographs of the deformed sample at various strain rates is shown in figure 2. During the compression, the barrelling effect is seen in the sample, which results in increase area at the centre of the sample. The extent of the damage, as seen in the radiograph is significantly larger at higher strain rates. The corresponding 3D rendering for the sample without deformation and 2×10^{-3}/s case is shown in figure 3.

The stress-strain behaviour for ADC12 and MADC12 at 60±5% solid fraction for MADC12 alloy is shown in figure 4. The stress strain curve can be divided into two zones. In zone one, there is a sharp increase in load followed by a slight decrease. This zone follows what is called as compaction mode, and in which dilatancy is observed. When the sample is subjected to loading, the grains pin up against each other (strain localization). This is indicated by the initial peak in the stress strain curve. The strain localization has been observed by Cai et.al [17], who had used Digital Image Correlation to quantify it. This is followed by a movement of grains to relieve stress, and inter dendritic liquid filling the voids formed by the movement of these grains, as indicated by the drop in the peak stress. There is a large change in stress for small change in strain. In the second zone, called the flow mode zone the solid starts flowing under a constant stress as indicated in the curve.

It was observed that the strain value at which peak stress occurs shifts to a higher value with increased strain rate (0.06048 for 2×10^{-4}/s, 0.22167, for 0.02/s). During 2×10^{-4}/s strain, the liquid flow due to a local pressure differential is comparable to that of the loading rate, and thus the peak stress value is significantly smaller at a lower strain value. With increasing the loading rate to 2×10^{-2}/s, the liquid flow lags behind, and the strain value for the peak stress increases. Thus the interplay between deformation

rate and the local strain values which determine the response of the interdendrtic liquid is vital to understand the crack formation during casting.

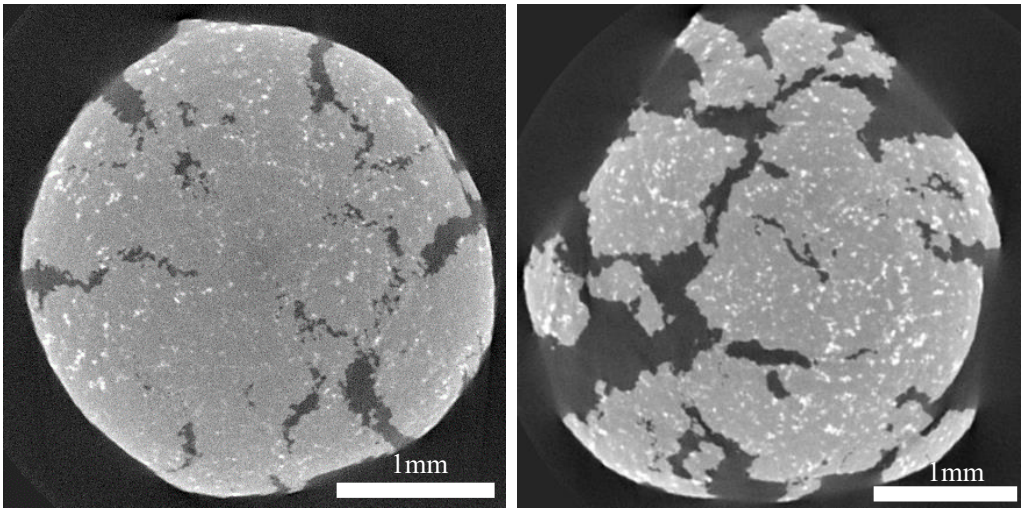

2×10^{-4}/s 2×10^{-2}/s

Figure 2: Radiographs of the deformed sample at (a) 2×10^{-4}/s (b) 2×10^{-3}/s and (c) 2×10^{-2}/s strain rate

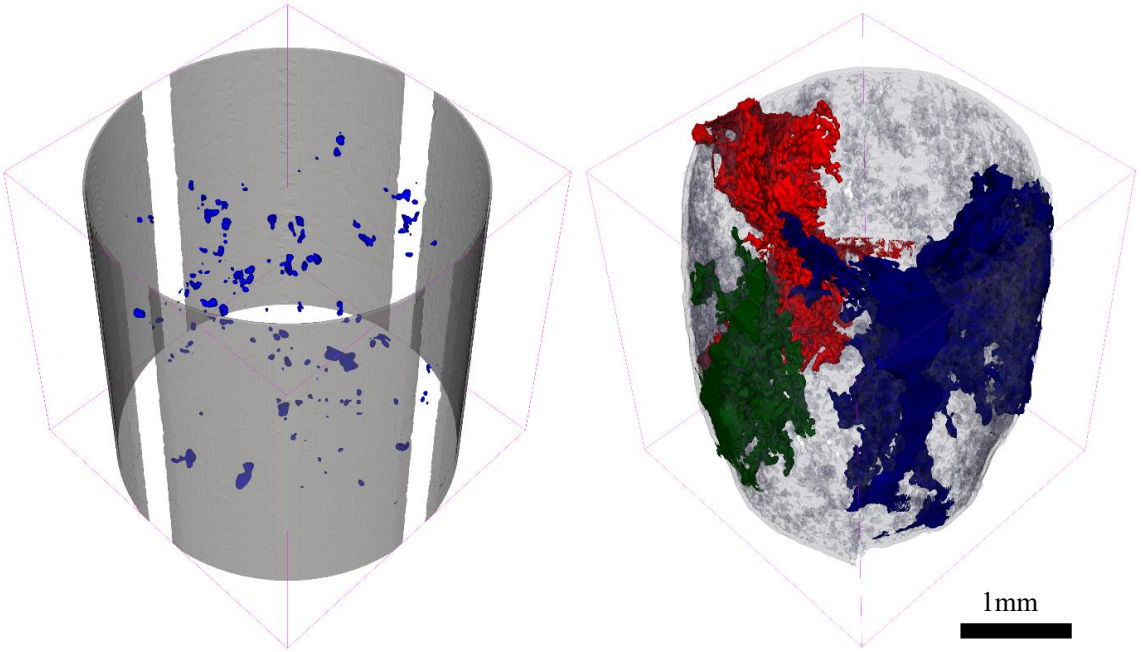

Figure 3: 3D rendering of the sample before and after deformation at 2×10^{-3}/s

The effect of temperature on ultimate compression load at 2×10^{-3}/s strain rate for ADC12 is shown in the figure 5. The behaviour of stress strain behaviour at 60% is explained in the previous section. With the increase in the solid fraction to 75%, the stress initially increases, but remains largely constant after that. However for the samples with 88% and there on the load increased continuously. This can be attributed to the formation of coherent dendritic network and on the application of load the dendrites move and entangle thus resisting the applied force.

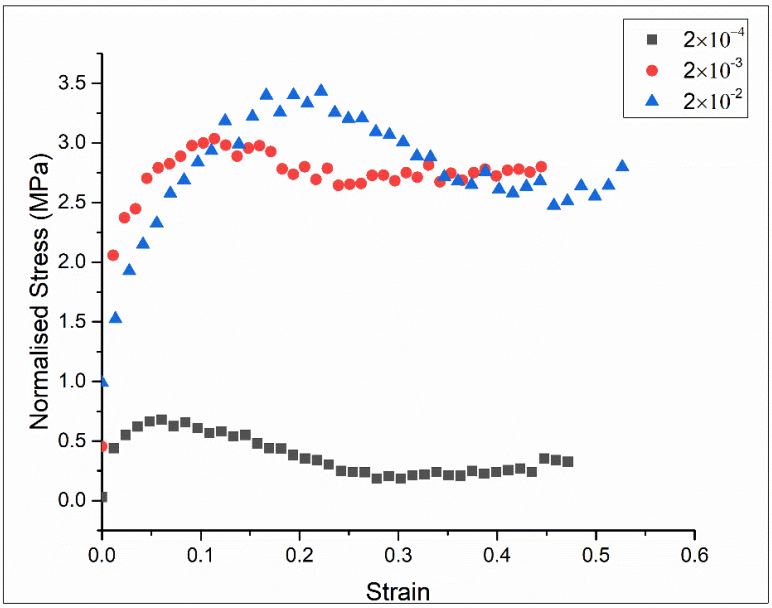

Figure 4: Influence of strain rates on the stress-strain behaviour at 60±5% solid fraction for the modified alloy

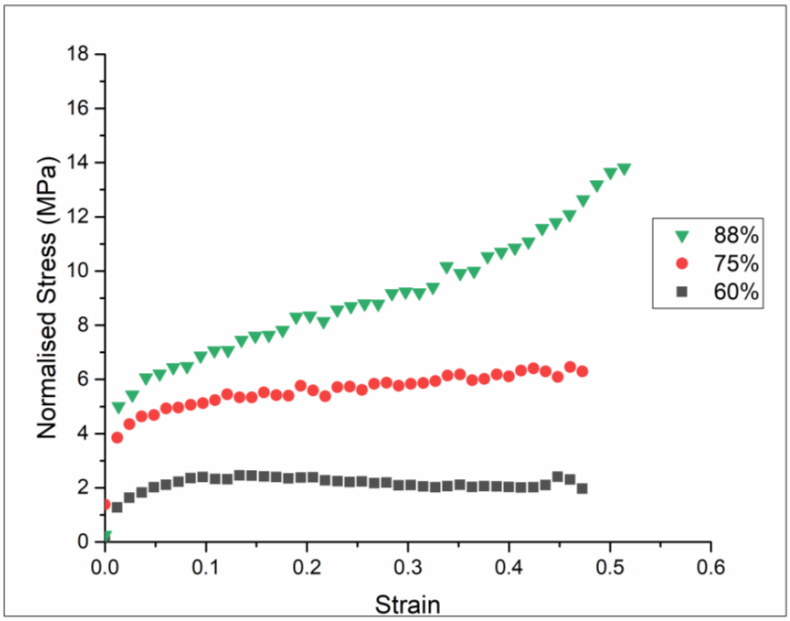

Figure 5: Influence of solid fraction on the stress-strain behaviour at 2×10^{-3}/s strain rate for ADC-12

4. Conclusion

The ADC12 alloy and the modified ADC12 alloy were subjected to the semisolid compression load to study the role of strain rates. The deformed sample was characterized in 3D using X-Ray tomography technique. This was followed by *in situ* experimentation by utilizing ultrafast synchrotron X-ray imaging to observe the hot crack formation 2 different Al-Si-Cu based die cast alloy specimens *in situ.* From, parametric studies the stress strain curve for ADC12 and MADC12 sample showed a characteristic hump followed by a constant stress region. The strain value at which peak stress occurs was found to shift to a higher value with increased strain rate. This was attributed to the competing deformation rate and liquid flow due to dilatancy.

Acknowledgement
SB is grateful to Dr. Sara Nonni, and Sebastian Marucci for their help during the experiments. The support from ferrous metallurgy lab and Machine tools lab, IIT Bombay in preparing samples is appreciated. Authors thank Ford USA for their partial financial support.

Reference

[1] Jason, Rowe P K M 2012 *Advanced materials in automotive engineering* ed R Jason (Woodhead Publishing Limited)
[2] Eskin D G, Suyitno and Katgerman L 2004 Mechanical properties in the semi-solid state and hot tearing of aluminium alloys *Prog. Mater. Sci.* **49** 629–711
[3] Puncreobutr C, Lee P D, Kareh K M, Connolley T, Fife J L and Phillion A B 2014 Influence of Fe-rich intermetallics on solidification defects in Al-Si-Cu alloys *Acta Mater.* **68** 42–51
[4] Gourlay C M, Dahle A K and Laukli H I 2004 Segregation band formation in Al-Si die castings *Metall. Mater. Trans. A* **35** 2881–91
[5] Lee P D and Hunt J D 2001 Hydrogen porosity in directionally solidified aluminium-copper alloys: A mathematical model *Acta Mater.* **49** 1383–98
[6] Terzi S, Salvo L, Suéry M, Limodin N, Adrien J, Maire E, Pannier Y, Bornert M, Bernard D, Felberbaum M, Rappaz M and Boller E 2009 In situ X-ray tomography observation of inhomogeneous deformation in semi-solid aluminium alloys *Scr. Mater.* **61** 449–52
[7] Gourlay C M and Dahle a K 2007 Dilatant shear bands in solidifying metals. *Nature* **445** 70–3
[8] Kim W Y, Kang C G and Kim B M 2007 Deformation behavior of wrought aluminum alloys in incremental compression experiment with a closed die *J. Mater. Process. Technol.* **191** 372–6
[9] Kang C G, Choi J S and Kim K H 1999 Effect of strain rate on macroscopic behavior in the compression forming of semi-solid aluminum alloy *J. Mater. Process. Technol.* **88** 159–68
[10] Kapranos P, Liu T Y, Atkinson H V. and Kirkwood D H 2001 Investigation into the rapid compression of semi-solid alloy slugs *J. Mater. Process. Technol.* **111** 31–6
[11] Tzimas E and Zavaliangos A 1999 Mechanical behavior of alloys with equiaxed microstructure in the semisolid state at high solid content *Acta Mater.* **47** 517–28
[12] Rappaz M, Drezet J M and Gremaud M 1999 A new hot-tearing criterion *Metall. Mater. Trans. A Phys. Metall. Mater. Sci.* **30** 449–55
[13] Sistaninia M, Phillion A B, Drezet J M and Rappaz M 2011 Simulation of semi-solid material mechanical behavior using a combined discrete/finite element method *Metall. Mater. Trans. A Phys. Metall. Mater. Sci.* **42** 239–48
[14] Cai B, Lee P D, Karagadde S, Marrow T J and Connolley T 2016 Time-resolved synchrotron tomographic quantification of deformation during indentation of an equiaxed semi-solid granular alloy *Acta Mater.* **105** 338–46
[15] Schindelin J, Arganda-Carreras I, Frise E, Kaynig V, Longair M, Pietzsch T, Preibisch S, Rueden C, Saalfeld S, Schmid B, Tinevez J Y, White D J, Hartenstein V, Eliceiri K, Tomancak P and Cardona A 2012 Fiji: An open-source platform for biological-image analysis *Nat. Methods* **9** 676–82
[16] Arganda-Carreras I, Kaynig V, Rueden C, Eliceiri K W, Schindelin J, Cardona A and Seung H S 2017 Trainable Weka Segmentation: A machine learning tool for microscopy pixel classification *Bioinformatics* **33** 2424–6
[17] Cai B, Karagadde S, Marrow T J, Connolley T and Lee P D 2015 Synchrotron X-ray tomographic quantification of deformation induced strain localisation in semi-solid Al-15wt.%Cu *IOP Conf. Ser. Mater. Sci. Eng.* **84**